MODELING METRIC DISTANCES OF DENDRITE SPINES OF MICE BASED ON MORPHOMETRIC MEASURES

E. Ceyhan[1], R.Ç. Ölken[1], L. Fong[2], T. N. Tasky[3], M. K. Hurdal[4], M. F. Beg[5], M. E. Martone[2], J. T. Ratnanather[3,6]*

[1]*Dept. of Mathematics, Koç University, 34450, Sarıyer, Istanbul, Turkey*
*corresponding author: phone: +90 (212) 338-1845, fax: +90 (212) 338-1559,
email: elceyhan@ku.edu.tr, web: http://home.ku.edu.tr/~elceyhan
[2]*Department of Neurosciences, University of California, San Diego, CA, 92093, USA*
[3]*Center for Imaging Science, The Johns Hopkins University, Baltimore, MD, 21218, USA*
[4]*Department of Mathematics, Florida State University, Tallahassee, FL 32306-4510, USA*
[5]*School of Engineering Science, Simon Fraser University, Burnaby, BC, V5A 1S6, Canada*
[6]*Institute for Computational Medicine, The Johns Hopkins University, Baltimore, MD, 21218, USA*

ABSTRACT

In this article, we model the metric distances of dendrite spines of mice based on various morphometric (shape and size related) measures, condition, and type of the spines. The question of interest is how the metric distances differ with respect to various morphometric measures, two different conditions and six spine types which are based on pre-assigned shape categories. Large Deformation Diffeomorphic Metric Mapping algorithm is one of the tools to measure morphometric differences in dendrite spines with respect to a template spine. We use Principal Component Analysis (PCA) on continuous numerical morphometric measures to obtain uncorrelated morphometric features, since PCA provides the orthogonal directions with most variation. We demonstrate that for the raw scores (i.e., values not adjusted for scale) metric distances differ significantly by size and type of spines, and size and length at each spine type level. Since size (or scale) dominates the other variables in variance and spine type is based on shape, differences in metric distances due to other variables might be masked. Hence, we adjust metric distances and other morphometric measures for scale. We demonstrate that after adjusting for scale, metric distances differ most significantly by shape (i.e., spine type), and then by length and size for each spine type. In the presence of other morphometric measures, the condition seems not to be significant in explaining variation in metric distances, hence we need to analyze spines for each shape type separately. Although the methodology used here is applied on morphometric measures of mouse spines, it is also valid for morphometric measures of other organs or tissues and other metric distances.

1 INTRODUCTION

The *Large Deformation Diffeomorphic Metric Mapping* (LDDMM) is a recently developed tool that quantizes morphometric (shape and size) differences between two binary images. This approach has been applied to the analysis of gross brain morphology derived from magnetic resonance imaging (MRI). Here, we apply this technique to the quantification of shape changes of microscopic structures, the tiny protuberances found on many types of neurons termed dendritic spines. Changes in dendritic spine size, shape and number are thought to underlie the brain's ability to change as a result of environmental stimulation and also occur in many pathological conditions. Thus, the quantification of shape changes in dendritic spines is a fundamental problem in neuroscience. A previous version of this data (with fewer dendrite spines) was analyzed in [1] wherein a linear model was fit on metric distances versus other variables such as volume, surface area, and length values. In [1], first statistical analysis was performed on metric distances and condition only. The dendritic spines were not matched for size and type of spine, so such factors might have caused the group differences in the metric distances, rather than the condition. Hence, other variables were included in the analysis. A linear model was fit with metric distances as the response variable and condition, type, volume, surface area, and length as predictor variables. In this work, the influence of the condition on the metric distances was analyzed after the influence of the type of spine, volume, surface area, and length was accounted for. Instead of running a linear model, we perform a *Principal Component Analysis* (PCA) to save all relevant information contained in the raw but correlated variables in a set of uncorrelated variables as much as possible. Then we identify the principal components (PCs) and use them as predictors in our linear models with metric distance being the response variable. The objective of this work is to determine the morphometric information conveyed by volume, surface area, and length, and whether the condition (disease), spine type (based on visual inspection of the morphometry),

morphometric features of dendritic spines in mice affect metric distances (with respect to a template spine). We also explore the affects of scaling on metric distances and on the results of our analysis.

Methods developed in the field of *Computational Anatomy* (CA) that enable quantification of anatomical volumes and shapes between and within groups of individuals with and without various neurological diseases have emerged from several groups in recent years ([7], [9], [13], [14], [20], [21], [22]). Based on the mathematical principles of general pattern theory ([5], [9]), these methods combine image-based diffeomorphic maps between MR scans with representations of anatomical shapes as smooth manifolds.

An important task in CA is the study of neuroanatomical variability [9]. The anatomic model is a quadruple $(\Omega, \mathrm{G}, \mathrm{I}, \mathrm{P})$ consisting of Ω the template coordinate space (in $\mathbf{R}^3$), defined as the union of 0, 1, 2, 3-dimensional manifolds, $\mathrm{G}: \Omega \leftrightarrow \Omega$ a set of diffeomorphic transformations on Ω, I the space of anatomies, is the orbit of a template anatomy I_0 under G, and P the family of probability measures on G. In this framework, a geodesic $\phi : [0,1] \to \mathrm{G}$ is computed where each point $\phi_t \in \mathrm{G}, t \in [0,1]$ is a diffeomorphism of the domain Ω. The evolution of the template image I_0 along path ϕ is given by $\phi_t I_0 = I_0 \circ \phi_t^{-1}$ such that the end point of the geodesic connects the template I_0 to the target I_1 via $I_1 = \phi_1 I_0 = I_0 \circ \phi_1^{-1}$. Thus, anatomical variability in the target is encoded by these geodesic transformations when a template is fixed.

Furthermore, geodesic curves induce metric distances between the template and the target shapes in the orbit. The diffeomorphisms are constructed as a flow of ordinary differential equations $\dot{\phi}_t = v_t(\phi_t)$, $t \in [0,1]$ with $\phi_0 = id$ the identity map, and associated vector fields $v_t, t \in [0,1]$. The optimal velocity vector field parameterizing the geodesic path is found by solving

$$\hat{v} = \underset{v:\phi = \int_0^1 v_t(\phi_t)\,dt,\, \phi_0 = id}{\arg\inf} \int_0^1 \|v_t\|_V^2 \, dt \text{ such that } I_0 \circ \phi_1^{-1} = I_1$$

where $v_t \in V$, the Hilbert space of smooth vector fields with norm $\|\cdot\|_V$ defined through a differential operator enforcing smoothness. The length of the minimal geodesic path through the space of transformations connecting the given anatomical configurations in I_0 and I_1 defines a metric distance, *D*, between anatomical shapes in I_0 and I_1 via

$$D(I_0, I_1) = \int_0^1 \|\hat{v}_t\|_V \, dt$$

where $\hat{v}_t$ is the optimizer calculated from the LDDMM algorithm ([2]). The construction of such a metric space allows one to quantify similarities and differences between anatomical shapes in the orbit. This is the vision laid out by D'Arcy W. Thompson more than one hundred years ago ([19]).

The notion of mathematical biomarker in the form of metric distance can be used in different ways. One is to generate metric distances of shapes relative to a template ([16], [2]). Another is to generate metric distances between each shape within a collection ([15]). The latter approach allows for sophisticated pattern classification analysis but is computationally expensive. We adopt the former approach here.

Previously, we demonstrated ([1]) that almost all of the variation in the metric distances could be explained by just $V^{1/3}$, $S^{1/2}$ and *L* where *V, S*, and *L* are volume, surface area, and length, respectively. That is, the size of the dendrites was shown to have the largest effect on the metric distances. However, the size differences could be masking the influence of other factors, such as the condition of mice. To this end, when data is scaled, the condition was significant after accounting for scaled *V, S*, and *L*, and type of spine.

In this article, we first consider the PCA of the numerical morphometric variables (*V, S*, and *L*), which is a way of identifying patterns in data, and expressing the data in such a way as to highlight their similarities and differences. In general, PCA is used for dimension reduction for multivariate data. However, we do not use PCA for this purpose, but to obtain a set of uncorrelated variables which measure different aspects of the morphometry of the dendrite spines that are identifiable in the PCs.

Then we use multiple linear regression on metric distances versus the PCs and other (categorical) variables to (i) understand which predictors have the greatest effect on metric distances, (ii) know the direction and magnitude of the effect, (iii) use the model to predict future values of the response when only the predictors are known. For variable selection, we perform a stepwise regression with backward elimination procedure ([4]).

2 DATA ACQUISITION

Pyramidial cells from layer V of primary visual cortex from genetically modified and control mice were injected with Lucifer yellow. Tissue was subse-

quently photo-oxidized and prepared for electron microscopy. 411 triangulated surface reconstructions of spine dendrites were produced by manual contouring of tomographic reconstructions of neurons and curated at the Cell-Centered DataBase at https://ccdb.ucsd.edu/CCDB/index.shtml ([11], [12]). The reconstructed spines were aligned with a standard coordinate system with respect to the smallest *Wild Type* (WT) spine via similitude matching (scale or no-scale, rotation, translation) of 14 landmarks suitably placed on each spine. LDDMM was applied to binarized images of the surfaces from which metric distances between the spines and the template (reference) spine were generated ([2]).

Variables include spine number, mouse number, shaft number, shaft label, condition, *V*, *S*, metric distance (*D*) values, *L*, and classification category (i.e., type of spines). *Condition of Mice* refers to whether the spine originated from a WT mouse or a genetically modified mouse. The WT mice are expected to have a normal genetic make-up because they originate from natural mice populations. However, in the *Knock-Out* (KO) mice, one specific gene is inactivated in order to mimic a human neurological condition. The six spine types are *double, filopodia, long mushroom, mushroom, stubby,* and *thin* ([10]). *V* is measured in μm^3, and *S* in μm^2. *L*, is the Euclidean distance between the neck landmark at the point closest to the dendrite shaft and the head landmark at the point furthest from the dendrite shaft and is measured in μm (micron or micrometer).

3 RESULTS

3.1 Analysis of Unscaled Morphometric Measures

First, we consider the unscaled numerical variables, namely, metric distance, volume, surface area, and length measures. These variables are significantly (positively) correlated with each other, with volume and surface area having the largest correlation coefficient (Pearson's $r = .95$ with $p < .0001$ for the alternative that the correlation coefficient is zero). See Table 1 for the corresponding (Pearson's) correlation coefficients and the *p*-values (given in parentheses) and Figure 1 for the pair plots of these variables. Therefore, when we use these raw variables in our model as predictors, there will be multicollinearity between the predictor variables, and one's presence in the model will render the other two variables insignificant. However, volume is mostly a measure of size, surface area is a measure of shape and size (but more of a measure of shape than size), and length is a measure associated with type of spine. Therefore, when one of the variables volume, surface area, or length is dismissed from the model, some important morphometric information about dendrite spines may be lost. To avoid this information loss, we perform PCA on volume, surface area, and length variables.

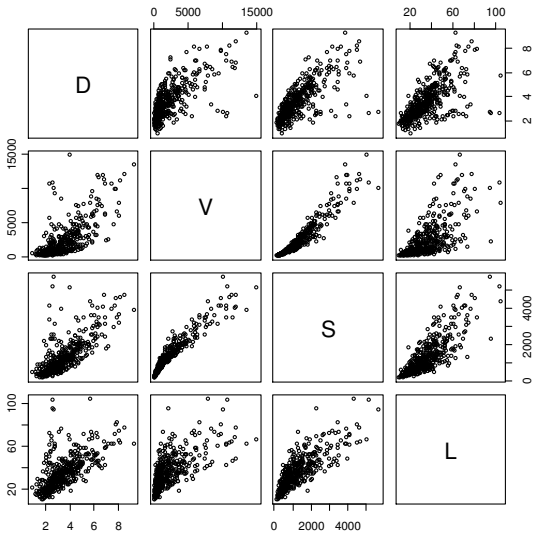

Figure 1: Pairs plot of the variables: metric distances (*D*), volume (*V*), surface area (*S*), and length (*L*).

In general, PCA can be performed on the correlation or covariance matrix (between the variables). PCA is performed on the covariance matrix if the variables are of similar scale or in same units of measurement; and on the correlation matrix for variables in different scales, as is the case here, since the measurements are in different units. Among variables in different scales (units), the variables with the larger variances (spread) dominate the PCA, thereby dominating the variables of import in smaller scales. However, it is not always the first PC that is of most interest, as the subsequent PCs might provide more important information in regard to the goal of the researcher ([8]). On the other hand, with such a standardization of the variables by using correlation matrix, once again crucial information loss could occur, as the spread in a variable could not merely be a by-product of scaling or difference in units. A middle way is to convert all variables to the same unit, if possible, and then apply PCA to the transformed variables. If we use $V^{1/3}$, $S^{1/2}$ and *L*, then all three variables will be of the same unit, namely μm. In our analysis, we apply PCA to obtain uncorrelated measures of morphometric features of dendrite spines rather than dimension reduction. So, we keep all the PCs resulting from the PCA procedure. Therefore, in our analysis, we prefer the PCA method with the best interpretability of the PCs.

dure on the resulting model ([4]). We stop the elimination procedure when all the remaining variables are significant at α=.05 level. Then we insert the spine type variable and its interaction with these remaining (significant) variables. We repeat the same variable selection (i.e., *stepwise backward elimination*) procedure on this new model. When all variables are significant, we stop the elimination procedure. The resulting model is

$$D_{ij} = \mu + \alpha_i^T + \left(\beta_0 + \beta_i^T\right) X_{ij}^{tPC1} + \gamma_i^T X_{ij}^{PC3} + \varepsilon_{ij}$$

where D_{ij} is the distance for spine *j* for type *i* (*i*=1 for double, 2 for filopodia, 3 for long mushroom, 4 for mushroom, 5 for stubby, and 6 for thin), X_{ij}^{tPC1} is the transformed *PC*1 score for spine *j* of type *i*, X_{ij}^{PC3} is the *PC*3 score for spine *j* of type *i*, μ is the overall mean, α_i^T is the effect of spine type level *i*, β_0 is the overall slope for transformed *PC*1 score, β_i^T is the slope of transformed *PC*1 score for spine type *i*, γ_i^T is the slope of transformed *PC*3 score for spine type *i*, and ε_{ij} is the error term. The adjusted R^2 value is 0.73 for this model. Furthermore, the residuals are not significantly non-normal (p= 0.0557 with Shapiro-Wilk normality test) and there is not significant autocorrelation between residuals (p= 0.5466 with Durbin-Watson test) ([17]).

Therefore, *tPC*1 (i.e., size component), spine type, and *tPC*1 by spine type interaction and *PC*3 by spine type interaction explain almost all of the variation in metric distances (73 %). However, differences in shape could be masked by the scale of the data, which is mostly conveyed by the size of the dendrite spines. Furthermore, types of spines were visually determined categories of shape, hence its presence could render *PC*2 (shape component) insignificant.

3.2 Analysis of Scaled Morphometric Measures

To overcome the highly dominant effect of scale (or size), we adjust the morphometric measures by scaling the metric distances, volumes, surface areas, and length measures. We obtain the scaled metric distances by applying the LDDMM algorithm to the scaled data (spines) rather than the distances that could be construed by scaling all the metric distances. The scaled metric distances are significantly negatively correlated with scaled volume and surface area measures, and scaled volumes and surface areas are significantly positively correlated. All other correlations are either mild or insignificant. See Table 3 for the corresponding correlation coefficients and the *p*-values (given in parentheses). Pairwise plots in Figure 4 also indicate this relationship between the variables.

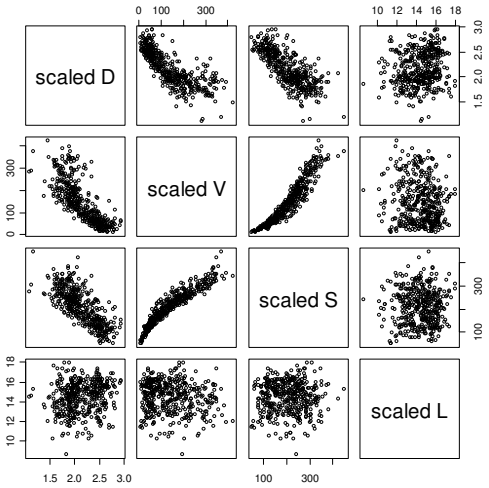

Figure 4: Pairs plot of the scaled morphometric measures.

As in the unscaled case, we apply three versions of PCA on the scaled variables. The corresponding factor loadings are presented in Table 4. For the purposes of interpretability of the *PC*s based on the scaled variables, denoted *sPC*s, we choose the third type, i.e., PCA on the variables transformed (to have the same unit). Looking at the table, we see that *sPC*1 is a measure of shape, *sPC*2 is of scaled length, while *sPC*3 is of scaled size. Observe that the scaling alters the order of importance of the variables, that is, before scaling, the order of variation in the variables were size > shape > length, while after scaling the order is shape > length > size. Running linear models with scaled *D* being the response and others being the predictors, one at a time, we see that each variable except spine category and condition is significant.

We transform the PC values as

$tsPC1 := \sqrt[3]{10 + sPC1 + |\min(sPC1)|}$,

$tsPC2 := \sqrt[3]{10 + sPC2 + |\min(sPC2)|}$, and

$tsPC3 := \sqrt[3]{10 + sPC3 + |\min(sPC3)|}$. Notice that to avoid negative PC values we add the absolute value of the minimum of each score and to reduce the positive skewness we add 10 to each score and then take the cube root. For the scatter plots of the metric distances of scaled spines versus transformed *sPC*1, *sPC*2, and *sPC*3, see Figure 5. Similar to the unscaled case, we start with the full model with all possible interactions, and perform the same model selection procedure. The resulting model is:

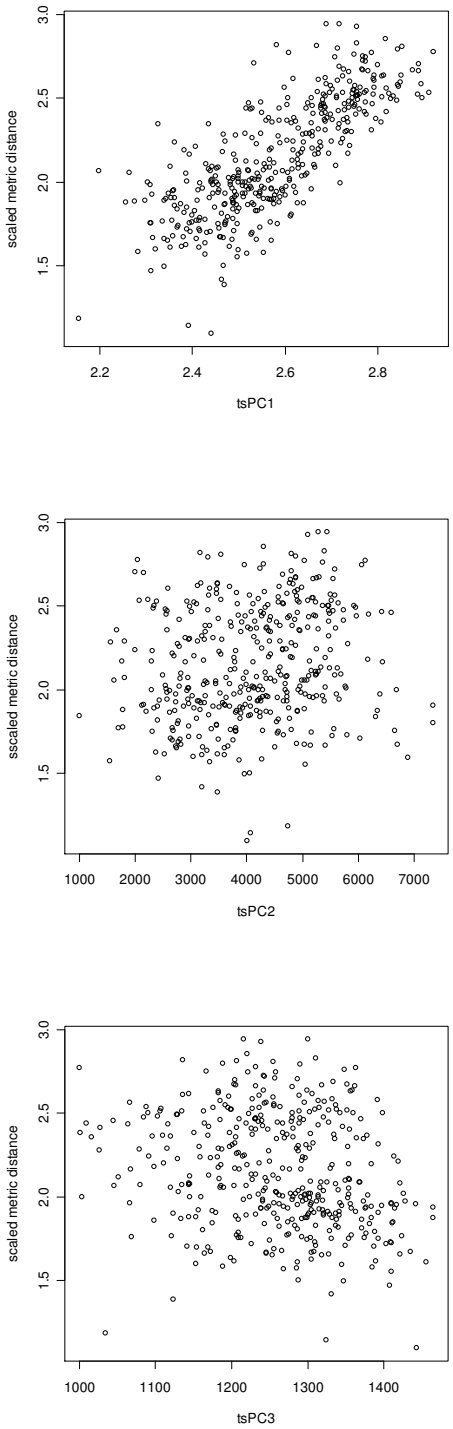

Figure 5: The scatter plots of the scaled metric distances versus transformed *sPC*1 *sPC*2, and *sPC*3.

$$D_{ij}^{s} = \mu^{s} + \alpha_{i}^{T,s} + \left(\beta_{0}^{s} + \beta_{i}^{T,s}\right) X_{ij}^{tsPC1} + \gamma_{i}^{T,s} X_{ij}^{sPC2} + \delta_{i}^{T,s} X_{ij}^{sPC3} + \varepsilon_{ij}^{s}$$

where D_{ij}^{s} is the scaled distance for spine *j* of type *i*, X_{ij}^{tsPC1} is the transformed *sPC*1 score for spine *j* of type *i*, X_{ij}^{sPC2} is the *sPC*2 score for spine *j* of type *i*, X_{ij}^{sPC3} is the *sPC*3 score for spine *j* of type *i*, μ^{s} is the overall mean, $\alpha_{i}^{T,s}$ is the effect of spine type level *i*, β_{0}^{s} is the overall slope for transformed *sPC*1 score, $\beta_{i}^{T,s}$ is the slope of transformed *sPC*1 score for spine type *i*, $\gamma_{i}^{T,s}$ is the slope of transformed *sPC*2 score for spine type *i*, $\delta_{i}^{T,s}$ is the slope of transformed *sPC*3 score for spine type *i*, and ε_{ij}^{s} is the error term (assumed to be distributed as iid $N(0,\sigma^2)$. The adjusted R^2 value 0.76 for this model. Moreover, the residuals are not significantly non-normal (p= 0.3217 based on Shapiro-Wilk normality test) and not significantly autocorrelated (p= 0.0771 based on Durbin-Watson test).

Therefore we observe that *sPC*1, spine type category, and interaction of spine type with all PCs are significant. That is, metric distances differ by shape and spine type category, and by length and size for each category.

4 DISCUSSION AND CONCLUSIONS

In this study, we used Large Deformation Diffeomorphic Metric Mapping (LDDMM) to generate metric distances to measure morphometric differences between dendrite spines of mice. We model the metric distances with respect to various other morphometric measures (such as volume, surface area, and length), condition (a genetic modification designed to mimic a human neurological condition versus healthy mice), and spine types. The disease condition does not significantly affect the metric distances in the presence of other morphometric measures and the spine type. But this does not mean that metric distances do not significantly differ with respect to the condition of mice, but rather metric distances are highly correlated with the other morphometric features, which ---when present in the model --- make the condition variable redundant. More precisely, morphometry of mice significantly differs due to the condition, but the variation in metric distances is mostly accounted for by the variation in other morphometric measures. We have also explored the effects of scaling on the morphometric

measures and their relation to metric distances. We demonstrate that metric distances are highly dependent on the morphometry and types of dendrite spines; and scaling changes the importance and order of this dependence. Therefore, computing metric distances with LDDMM is a powerful tool in detecting morphometric diffences between dendrite spines of various size and shape. However, to detect the differences due to the disease condition, we recommend a different set of analysis. Either, one could run a linear model with each morphometric variable (i.e., LDDMM metric distance, volume, surface area, and length) being the response, and condition and spine type being the predictor variables; or run a PCA on the morphometric variables and use each PC as the predictor with condition and spine being the response variables; or run MANOVA with all the morphometric variables being the response and condition and spine being the predictors.

Acknowledgements

Research was supported by NSF ACS-9619020, NSF DMS-0456253, NSF DMS-0101329, NIH P41-RR15241, NIH P20-EB02013, P41-RR04050, P41-RR08605, R01-DA016602 and NSERC 31-611387.

REFERENCES

[1] G. Aldridge, T. N. Tasky, J. T. Ratnanather, M. E. Martone, M. Terada, M. F. Beg, L. Fong, E. Ceyhan, A. E. Kolasny, T. Brown, E. L. Cochran, S. J. Tang, D. V. Pisano, M. Vaillant, M. K. Hurdal, J. D. Churchill, W. T. Greenough, M. I. Miller, and M. H. Ellisman (2005): Semi-automated shape analysis of dendrite spines from animal models of FragileX and Parkinson's Disease using Large Deformation Diffeomorphic Metric Mapping. Society for Neuroscience Annual Meeting, Washington DC, 2005. Available at_____ http://www.cis.jhu.edu/posters/sfn2005v2.pdf

[2] M. F. Beg, M. I. Miller, A. Trouve, and L. Younes (2005): Computing large deformation metric mappings via geodesic flows of diffeomorphisms. International Journal of Computer Vision 61:139-157.

[3] W. J. Burke, J. P. Miller, E. H. Rubin, J. C. Morris, L. A. Coben, J. Duchek, et al. (1988): Reliability of the Washington University Clinical Dementia Rating. Archives of Neurology 45:31-32.

[4] K. P. Burnham and D. Anderson (2003): Model Selection and Multi-Model Inference. New York: Springer.

[5] G. E. Christensen, R. D. Rabbitt, and M. I. Miller (1996): Deformable templates using large deformation kinematics. IEEE Transactions on Image Processing 5:1435-1447.

[6] W. J. Conover (1999): Practical Nonparametric Statistics, 3rd ed. New York: John Wiley & Sons.

[7] J. G. Csernansky, L. Wang, S. C. Joshi, J. T. Ratnanather, and M. I. Miller (2004): Computational anatomy and neuropsychiatric disease: Probabilistic assessment of variation and statistical inference of group difference, hemispheric asymmetry, and time-dependent change. NeuroImage 23:S56-S68.

[8] B. Everitt (2005): An R and S-Plus Companion to Multivariate Analysis: Springer Texts in Statistics.

[9] U. Grenander and M. I. Miller (1998): Computational anatomy: An emerging discipline. Quarterly of Applied Mathematics 56:617-694.

[10] K. M. Harris, F. E. Jensen, and B. Tsao. (1992) Three-dimensional structure of dendritic spines and synapses in rat hippocampus (CA1) at postnatal day 15 and adult ages: implications for the maturation of synaptic physiology and long-term potentiation. J. Neurosci. 12, 2685-2705.

[11] M. E. Martone, A. Gupta, M. Wong, X. Qian, G. Sosinsky, B. Ludäscher, and M. H. Ellisman (2002): A cell-centered database for electron tomographic data. Journal of Structural Biology 138, 145–155.

[12] M. E. Martone, S. Zhang, A. Gupta, X. Qian, D. L. Price, M. Wong, S. Santini, and M. H. Ellisman (2003): The cell-centered database: a database for multiscale structural and protein localization data from light and electron microscopy. Neuroinformatics 1, 379-395.

[13] M. I. Miller (2004): Computational anatomy: Shape, growth, and atrophy comparison via diffeomorphisms. NeuroImage 23:S19-S33.

[14] M. I. Miller, G. E. Christensen, Y. Amit, and U. Grenander (1993): Mathematical textbook of deformable neuroanatomies. Proceedings of the National Academy of Sciences of the United States of America 90:11944-11948.

[15] M. I. Miller, C. E. Priebe, B. Fischl, A. E. Kolasny, Y. Park, and R. L. Buckner, BIRN M (2006): Collaborative Computational Anatomy: The Perfect Storm for MRI Morphometry Study of the Human Brain via Diffeomorphic Metric Mapping, Multidimensional Scaling and Linear Discrminant Analysis. Proc. Nat. Acad. Sci. (submitted)

[16] M. I. Miller, A. Trouve, and L. Younes (2002): On the metrics and Euler-Lagrange equations of computational anatomy. Annual Review of Biomedical Engineering 4:375-405.

[17] G. A. F. Seber and A. J. Lee (2003): Linear Regression Analysis. New York: Wiley & Sons.

[18] H. C. Thode Jr. (2002): Testing for Normality. New York: Marcel Dekker.

[19] D. W. Thompson, (1992) "On Growth and Form: The Complete Revised Edition", New York, Dover.

[20] P. M. Thompson, K. M. Hayashi, E. R. Sowell, N Gogtay, J. N. Giedd, J. L. Rapoport, et al. (2004): Mapping cortical change in Alzheimer's disease, brain

development, and schizophrenia. Neuroimage 23:S2-S18.
[21] A. W. Toga (2005): Computational biology for visualization of brain structure. Anatomy and Embryology 210:433-438.
[22] A. W. Toga and P. M. Thompson (2005): Brain atlases of normal and diseased populations. Int Rev Neurobiol 66:1-54.

5 TABLES

	D	*V*	*S*	*L*
D	1.00	.70 (< .0001)	.72 (< .0001)	.64 (< .0001)
V	.70	1.00	.95 (< .0001)	.66 (< .0001)
S	.72	.95	1.00	.80 (< .0001)
L	.64	.66	.80	1.00

Table 1: Pearson's correlation coefficients between the (continuous) unscaled numerical morphometric variables; metric distances, volume, surface area, and length, and the corresponding *p*-values in parentheses.

	PCA on correlation of original variables			**PCA on covariance of original variables**			PCA on covariance of transformed variables		
	*PC*1	*PC*2	*PC*3	***PC*1**	***PC*2**	***PC*3**	*PC*1	*PC*2	*PC*3
V	-.58	.56	.60	**.94**	**.35**	**.00**	-.18	-.33	.93
S	-.61	.19	-.77	**.35**	**-.94**	**.00**	-.58	-.72	-.37
L	-.54	-.81	.23	**.00**	**.00**	**1.00**	-.79	.61	.00

Table 2: Factor loadings for original variables on the principal components resulting from the three types of PCA considered. The PCA we use in subsequent analysis is presented in bold face.

	Scaled *D*	Scaled *V*	Scaled *S*	Scaled *L*
Scaled *D*	1.00	-.78 (< .0001)	-.76 (< .0001)	.18 (.0001)
Scaled *V*	-.78	1.00	.94 (< .0001)	-.13 (.0039)
Scaled *S*	-.75	.94	1.00	-.01 (.4522)
Scaled *L*	.18	-.13	-.01	1.00

Table 3: Pearson's correlation coefficients between the (continuous) scaled (i.e., scale-adjusted) numerical morphometric variables; metric distances for scaled spines, scaled volume, scaled surface area, and scaled length measures and the corresponding *p*-values in parentheses.

	PCA on correlation of original variables			PCA on covariance of original variables			**PCA on covariance of transformed variables**		
	*sPC*1	*sPC*2	*sPC*3	*sPC*1	*sPC*2	*sPC*3	***sPC*1**	***sPC*2**	***sPC*3**
Scaled *V*	-.71	.00	.71	.78	.62	.00	**-.40**	**.00**	**.92**
Scaled *S*	-.70	.14	-.70	.62	-.78	.00	**-.92**	**.00**	**-.39**
Scaled *L*	.10	.99	.00	.00	.00	1.00	**.00**	**1.00**	**.00**

Table 4: Factor loadings for scaled original variables versus the PCs resulting from the three types of PCA considered. The PCA we use in subsequent analysis is presented in bold face.